

## METALLURGICAL STABILITY OF INCONEL ALLOY 718

J.W. Brooks and P.J. Bridges

Inco Engineered Products Limited  
Wiggin Street, Birmingham. B16 0AJ England

### Summary

Extensive heat treatment and forging trials have been carried out on INCONEL\* alloy 718 produced by modern vacuum melting practice in order to clarify the time-temperature transformation characteristics of the material. The effect of forging practice on microstructure and mechanical properties has also been determined together with the long term stability of the alloy.

The gamma star precipitation behaviour has been defined for annealing times up to 10,000 hours and the transformation kinetics have been compared and contrasted with those of conventional gamma prime strengthened superalloys. The work described provides an explanation for the relationship between grain boundary delta precipitation and creep ductility.

## Introduction

The use of INCONEL alloy 718 as a disc material in gas turbine engines has increased significantly in recent years as it has good properties up to 650°C and is competitively priced due to the fact that the alloy contains no cobalt and has a relatively high iron content. However the material was originally developed as a weldable sheet alloy for service at intermediate temperatures and therefore much of the early work is not relevant to the current applications. Furthermore the data available on the precipitation reactions is ambiguous and is not sufficient to account for the behaviour of the alloy in service. Thus the aim of the work discussed in this paper was to define fully the microstructural effects of forging practice and heat treatment.

## Experimental

The material used was commercially produced (INCO ALLOYS INTERNATIONAL LTD.) vacuum melted and refined alloy 718, homogenised and side forged down to 100mm diameter bar. The effects of solution treatment temperature (from 950 to 1200°C) and cooling rate (water quench, air cool or furnace cool) were investigated prior to isothermal annealing (0.1 to 10,000 hours from 500 to 1000°C) to determine the time, temperature, transformation behaviour. Forging trials were carried out using a 3:1 reduction at temperatures between 940 and 1120°C with up to three reheat temperatures and four interstage anneals. After conventional heat treatment (using either 955 or 980°C solution treatments) the forgings were given full mechanical property and metallographic assessments.

Selected fully heat treated forgings were subjected to long term exposure for 1000 and 10,000 hours at 650°C and 10,000 hours at 575°C and the structure and properties were then re-evaluated.

Metallographic analysis was carried out using conventional optical techniques combined with scanning and transmission electron microscopy. Mechanical testing was carried out on samples machined from the discs and consisted of tensile tests at room temperature or 650°C together with smooth and notched stress rupture at 650°C (730MPa) or 705°C (415MPa).

## Results

### (a) Effect of Annealing

The precipitating phases were all based on Ni<sub>3</sub>Nb with varying amounts of titanium and aluminium substituting for the niobium. The principal strengthening phase was gamma star ( $\gamma^*$ , sometimes called  $\gamma''$  or gamma double prime) a body-centred tetragonal phase which formed as coherent platelets in three variants lying on the  $\{100\}$  planes of the face-centre cubic matrix. The most stable Ni<sub>3</sub>Nb precipitate was the orthorhombic delta phase which nucleated at grain boundaries and grew into plates lying on the matrix  $\{111\}$  planes. Gamma prime ( $\gamma'$ ) precipitates with the usual L1<sub>2</sub> structure were also observed, usually in matrix material which was niobium depleted due to heavy delta or  $\gamma^*$  precipitation. Similarly body-centred cubic alpha chromium ( $\alpha$ -Cr) formed as globular particles at grain boundaries when the matrix became nickel depleted due to extensive precipitation of the intermetallic phases.

Solution treatment below 1010°C gave rise to delta phase while grain growth occurred above 1060°C although for fine grained material (<ASTM 7) grain growth started at 1020°C. The titanium and niobium primary carbides, which form during solidification, were stable throughout the temperature range examined and no evidence was found for the formation of Laves phase even at the highest temperature. It was found that variations in cooling rate from the solution treatment temperature had a marked influence on the kinetics of subsequent precipitation of the  $\gamma^*$  phase during ageing. In particular rapid quenching enhanced the ageing response while slow cooling produced precipitation in the solution treated condition. Intermediate cooling rates suppressed precipitation but also reduced the nucleation kinetics. (Figure 1)

The long term exposure work showed that the  $\gamma^*$  was stable, for 10,000 hours at 600°C, with very little particle coarsening. However, at higher temperatures and for times in excess of 3000 hours the  $\gamma^*$  decomposed to form either  $\gamma'$  (650-850°C) or delta (750-1000°C). Also small quantities of globular  $\delta$ -chromium particles were observed, mainly at the grain boundaries, after 3000 hours at intermediate temperatures.

The t-t-t characteristics of these phases are shown in Figure 2. However, the formation of the  $\delta$ -chromium is very dependent on the stress state of the material and can form at much shorter times under creep conditions. Similarly  $M_6C$  does not form after annealing but was observed in samples deformed at temperature.

In an attempt to establish the precipitation kinetics the volume fractions of the  $\gamma^*$  phase, formed during ageing at 700°C, were determined using both geometrical methods and microanalytical techniques. For comparison purposes, measurements were also carried out on NIMONIC\* alloy 901, which has a similar composition to alloy 718 but is precipitation hardened with  $Ni_3(Al,Ti)$   $\gamma'$  particles. The results are shown in Figure 3 and it is clear that the ageing responses are quite different such that the  $\gamma^*$  precipitate volume fraction and size increase with time while the  $\gamma'$  coarsens with a constant volume fraction. In both cases particle coarsening follows the  $t \propto d^3$  relationship observed in other nickel base materials (t is time and d is particle diameter).

#### (b) Effect of Forging

Typical forged microstructures are shown in Figure 4 and the micrographs are arranged so that the effects of the different forging parameters can be examined independently. It was clear that the final grain size became smaller as the forging temperature was reduced while an increase in the number of stages (reheats) gave some further refinement to the overall structure. However, this was accompanied by some sporadic grain growth. The resulting duplex grain structure was typical of all the multi-stage forgings and was most apparent in those forgings done at the higher temperatures. The greatest microstructural refinement was obtained by a multi-stage forging route carried out at successively lower temperatures and finished below 1000°C. The structures observed after this type of processing were characterised by a fairly uniform grain size ( $\sim$  ASTM 10) with a fine distribution of the delta phase on the grain boundaries.

The 955°C solution treatment gave rise to fairly extensive grain boundary delta precipitation particularly in those samples which contained this phase in the as-forged condition. Annealing at 980°C, however, produced much smaller quantities of delta and tended to spheroidise that which was already present in the structure.

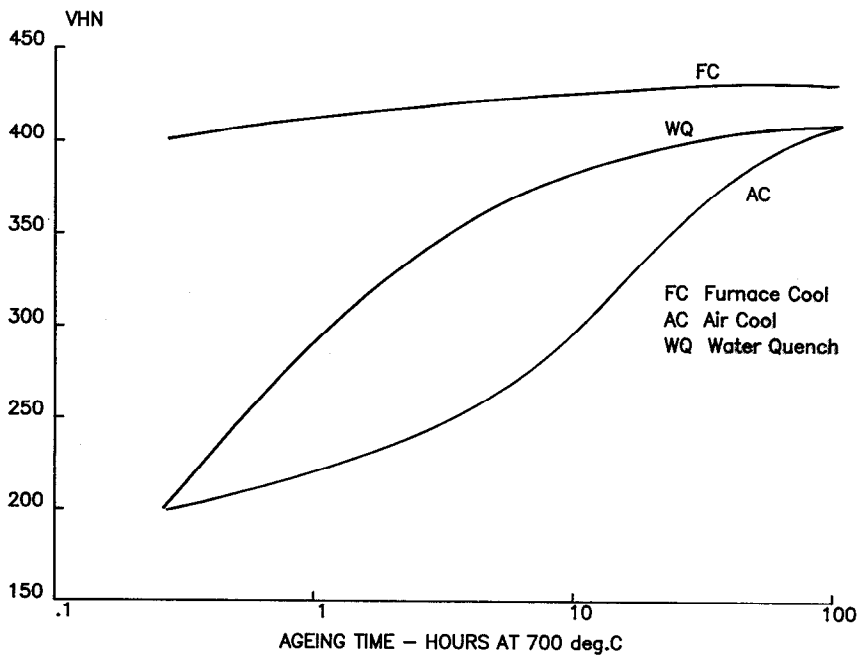


Figure 1

Ageing response after various cooling rates from 1060°C

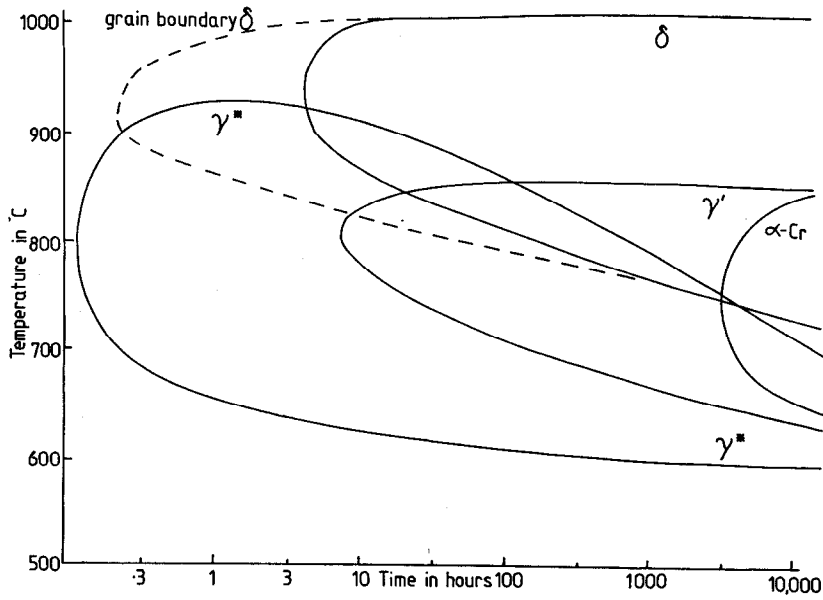


Figure 2

T-T-T curves

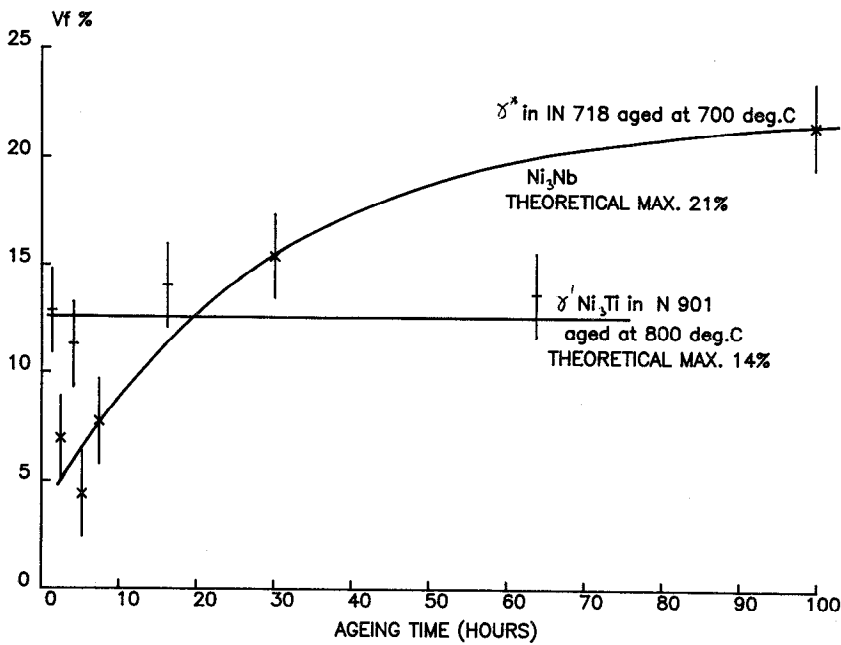
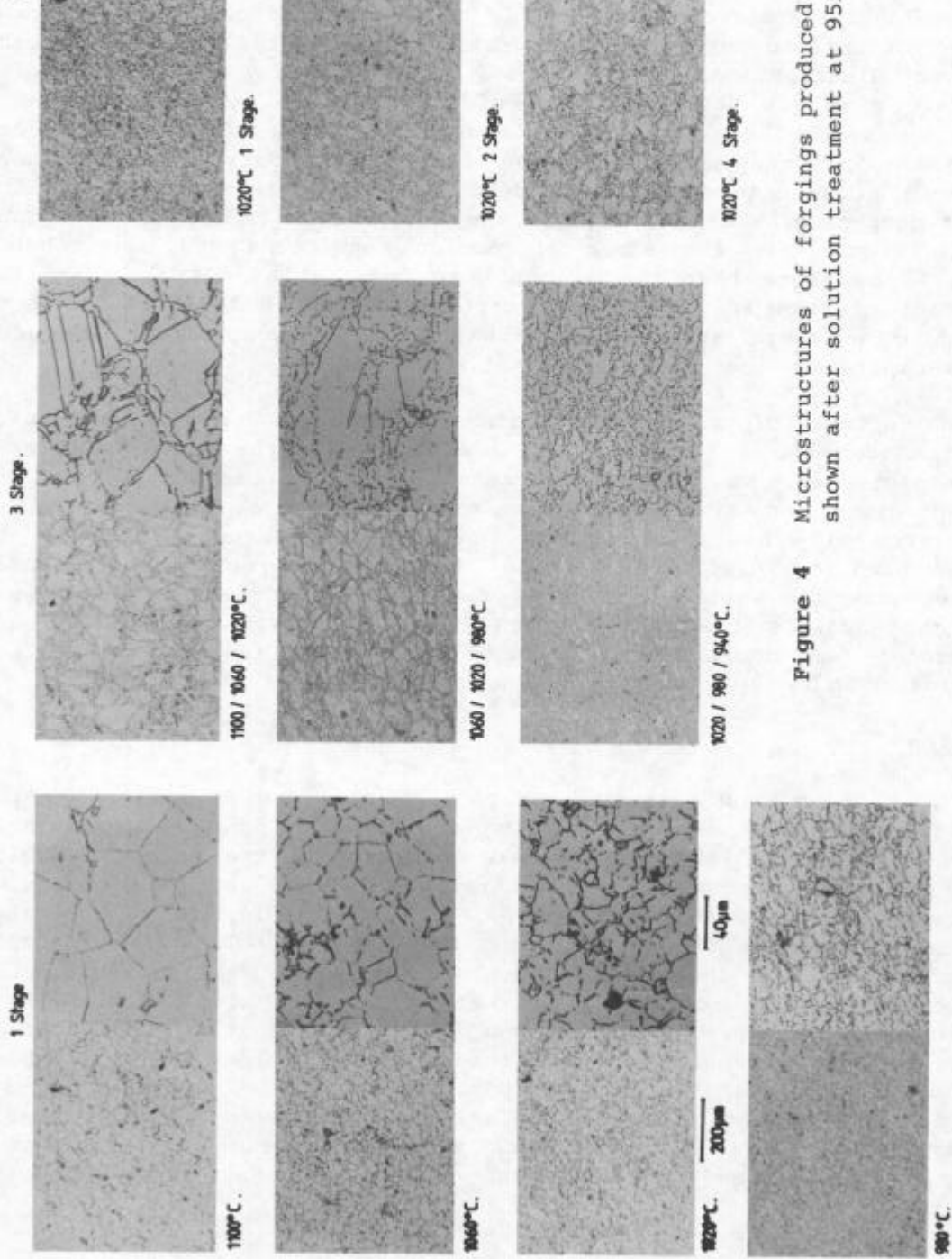


Figure 3

Volume fraction as a function of ageing time



**Figure 4** Microstructures of forgings produced shown after solution treatment at 95

The grain refinement which occurred during forging at lower temperatures gave increased tensile strength with slightly reduced ductility. In general the tensile properties were unaffected by the different delta morphologies associated with the 955 and 980°C anneals. The stress rupture properties, however, varied with both forging and solution treatment temperature. The coarse delta-free structures produced by high working and annealing temperatures were very notch sensitive although the lives were quite high. Notch strengthening together with good lives was obtained by finish forging at low temperatures to produce a uniform fine grain size with some grain boundary delta precipitation.

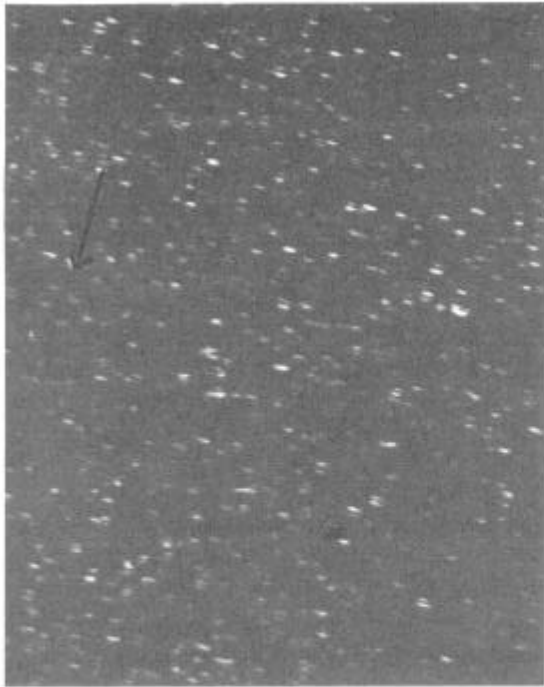
### (c) Effect of exposure

The optical microstructures of the forged discs before exposure consisted of uniform recrystallised grain structures of ASTM 8-11 together with even distributions of discrete grain boundary delta particles. This grain size was stable for all of the exposure conditions and this stability was also true of the intergranular delta phase although the precipitation in the samples exposed for 10,000 hours at 650°C showed evidence of coarsening with a tendency to form grain boundary films. The  $\gamma^*$  morphologies can be seen in the transmission electron micrographs shown in Figure 5. The same diffraction conditions and magnification were used to ensure that the images were comparable. It is clear that significant coarsening of the  $\gamma^*$  particles had taken place during the 10,000 hour exposure at 650°C and that this was concomitant with some  $\gamma'$  precipitation.

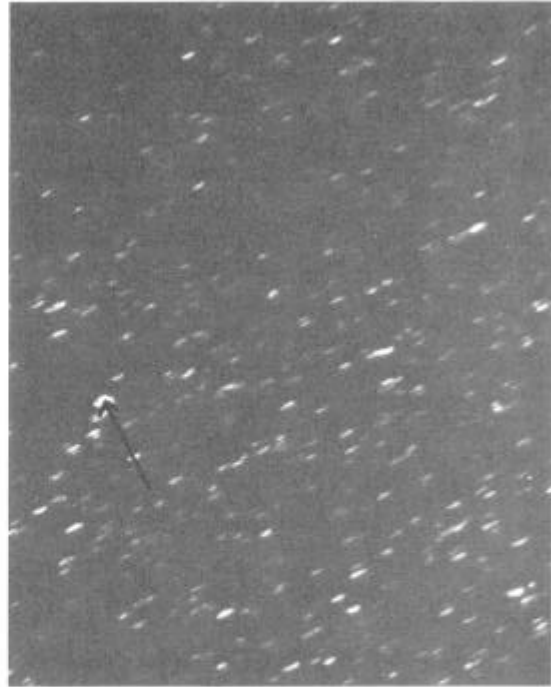
The effect of these microstructural changes on the mechanical properties is shown in Tables 1 and 2 which detail the tensile and creep data respectively. No significant variations were observed between the different discs and consequently the values quoted are averages of the results from all the test pieces. The coarse structure present in the sample exposed for 10,000 hours at 650°C resulted in a loss in both tensile and creep strength while ductilities were relatively unaffected. However the slight particle coarsening evident after exposure at 575°C increased both strength and ductility while 1000 hours at 650°C had little effect, in accordance with the minor microstructural changes.

### Discussion

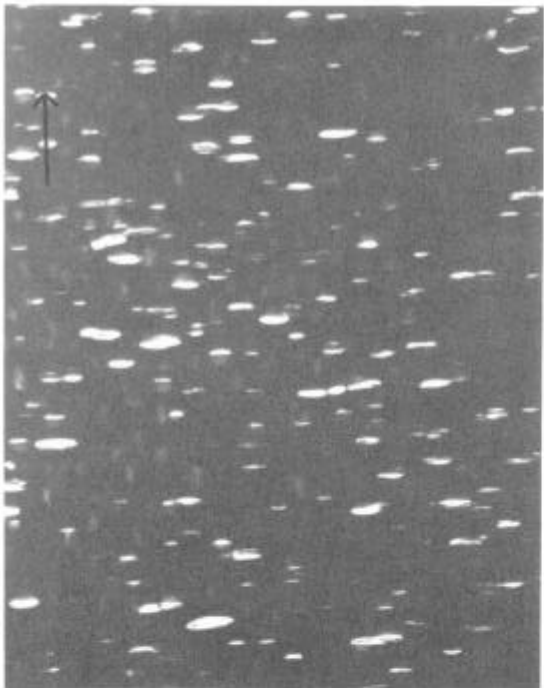
It is clear from this work that  $\gamma^*$ ,  $\gamma'$  and delta are the only phases to precipitate during annealing at 500-1000°C for up to 100 hours while no significant differences were observed in the primary carbides after solution treatment at temperatures up to 1200°C. No evidence was found for grain boundary carbide films, of either  $M_6C$  or  $NbC$ , or metallic precipitates such as  $\alpha$ -chromium or Laves phase. This is in marked contrast to some of the early literature (e.g. 1) but is supported by the later observations of Boesch and Canada (2) who showed that the Laves phase identified in previous work was probably delta. It is also likely that the greater susceptibility to carbide formation observed by Eiselstein was related to the higher carbon content of the air melted alloy used as compared to current vacuum melted material. It is not clear, however, how changes in  $NbC$  could take place anyway as these carbides form at high temperature, close to the solidus, and are very stable.



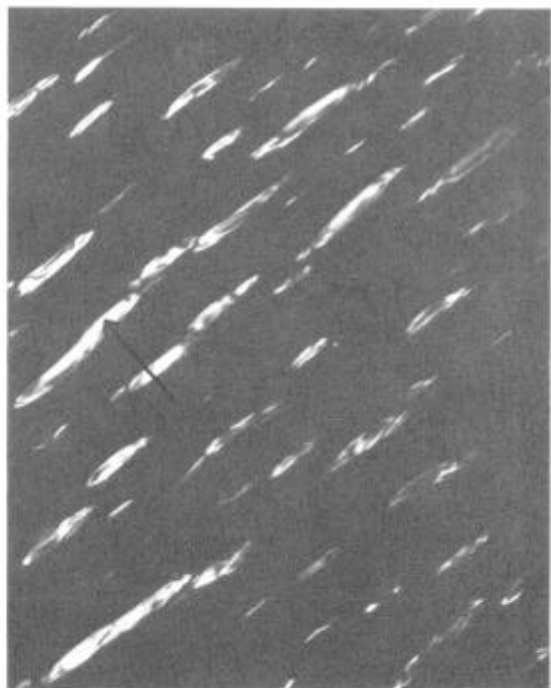
(a)



(b)



(c)



(d)

Figure 5 Effect of exposure on  $\gamma^*$

(a) As received

(b) 1,000 hours at 650°C

(c) 10,000 hours at 575°C

(d) 10,000 hours at 650°C

$g$  is 100,  $B \sim [001]$ ,  $\longleftrightarrow$  0.2  $\mu\text{m}$

**TABLE 1**  
Average Tensile Properties of Forged Discs  
after long term exposure

Exposure Conditions	Test Temp. °C	0.2% PS MPa	UTS MPa	El.%	R.ofA. %
1000 hrs. @ 650°C	RT	1182 ± 18	1450 ± 15	19.0 ± 1	33.6 ± 2
	650	987 ± 12	1188 ± 10	27.1 ± 2	60.7 ± 4
10,000hrs. @ 650°C	RT	1054 ± 19	1382 ± 9	18.1 ± 2	26.0 ± 2
	650	847 ± 4	1109 ± 13	28.3 ± 2	61.4 ± 4
10,000hrs. @ 575°C	RT	1233 ± 11	1441 ± 19	19.9 ± 2	34.6 ± 2
	650	1020 ± 8	1189 ± 16	23.8 ± 3	57.3 ± 4
Unexposed material	RT	1170 ± 20	1412 ± 14	19.0 ± 2	31.0 ± 5
	650	965 ± 13	1156 ± 9	25.3 ± 3	60.0 ± 4

**TABLE 2**  
Average creep rupture properties of forged discs after long term exposure

Exposure Conditions	Test Conditions	Life	Elong.
1000hrs. @ 650°C	730 MPa 650°C Notched	79	33.5
10,000hrs. @ 650°C	" " " "	11	31.0
10,000hrs. @ 575°C	" " " "	72	33.9
Unexposed material	" " " "	55	30.8
1000hrs. @ 650°C	415 MPa 705°C Plain	98	21.0
10,000hrs. @ 650°C	" " " "	69	32.8
10,000hrs. @ 575°C	" " " "	259	30.8
Unexposed material	" " " "	197	38.0



It can be seen that the three precipitation reactions observed, which are all based on  $\text{Ni}_3$  (Nb,Ti,Al) compounds are a complex function of time and temperature. In particular the growth rate and volume fraction of the primary age hardening phase, the  $\gamma^*$ , is very dependent on cooling rate from the solution treatment temperature and this could certainly account for the variable mechanical properties observed in some large complex parts. The faster nucleation and growth rates observed in the rapidly cooled samples are probably associated with enhanced diffusion due to the quenched-in supersaturation of vacancies. The  $\gamma^*$  coarsening rates correlated well with the values quoted in the literature (e.g. 3 and 4) while the volume fractions obtained were slightly higher. The latter effect is probably due to the chemical extraction techniques used in the previous work as these can readily underestimate volume fractions as a result of partially dissolving the phase under examination. It is believed that the slow increase in volume fraction of the  $\gamma^*$  in alloy 718, as compared to the  $\gamma'$  in alloy 901 which reaches a maximum very rapidly, is due to the low diffusivity of niobium in nickel.

Various values have been quoted (e.g. 5 and 6) for the relative amounts of  $\gamma^*$  and  $\gamma'$  present in alloy 718 aged at  $700^\circ\text{C}$  which range from 0.2 to 0.4 for the volume fraction ratio of  $\gamma'/\gamma^*$ . This implies that half of the precipitation imaged in a typical  $\langle 100 \rangle$  dark field micrograph should be  $\gamma'$  (as all the  $\gamma'$  but only one variant (i.e.  $1/3$ ) of the  $\gamma^*$  precipitates are in contrast) and this is clearly not true even of the images shown in the literature (e.g. 7). Generally  $\gamma'$  is differentiated from  $\gamma^*$  by imaging near the  $[001]$  zone axis (or crystallographically equivalent conditions) using  $010$ , to show  $\gamma'$  and  $\gamma^*$ , and  $1, \frac{1}{2}, 0$ , to just show  $\gamma^*$ , so that contrast present in the former image but not the latter is attributed to  $\gamma'$ . However at this beam direction, and using the same notation,  $010$  is also close to  $\frac{1}{2}, 1, 0$  and consequently faint contrast can arise from another  $\gamma^*$  variant and it is likely that this has been interpreted erroneously as  $\gamma'$ . The analysis carried out in this work did not show any  $\gamma'$  to be present after ageing at  $700^\circ\text{C}$  for up to 100 hours but  $\gamma'$  was observed after ageing at  $800^\circ\text{C}$  such that the  $\gamma'/\gamma^*$  volume fraction ratio was 0.2 after 100 hours (long term exposure data indicates that  $\gamma'$  can form at  $700^\circ\text{C}$  after 1000 hours). Clearly the susceptibility of alloy 718 to  $\gamma'$  precipitation is highly temperature dependent and is probably affected by slight composition differences. Thus the precipitation characteristics of the  $\text{Ni}_3\text{Nb}$   $\gamma^*$  phase present in alloy 718 are significantly different from those associated with the more commonly observed  $\text{Ni}_3$  (Ti,Al) $\gamma'$  precipitates present in the majority of superalloys since the kinetics are much slower. In particular the volume fraction of the  $\gamma^*$  precipitates produced on ageing between  $500^\circ\text{C}$  and  $700^\circ\text{C}$  increases substantially with annealing times up to 100 hours. An important consequence of this behaviour is that the conventional ageing treatment for alloy 718 does not produce the equilibrium structure, as the  $\gamma^*$  volume fraction is only  $\sim 13\%$  compared to a theoretical maximum of  $\sim 21\%$ . Thus it can be seen that the enhanced properties associated with long term exposure at  $575^\circ\text{C}$  are a result of increased precipitation without excessive particle growth while the degraded properties resulting from long times at  $650^\circ\text{C}$  are due to enhanced Oswald ripening at the higher temperature.

The principal failure mechanism in the test pieces was ductile and intergranular and the primary influence of thermal exposure was to soften further the grain boundary regions and so enhance the ductile appearance of the fracture. This grain boundary softening was the result of niobium depletion at the grain boundaries associated with the delta precipitation. Thermal exposure increases the depletion and eventually

gives rise to the formation of  $\delta$  ' zones adjacent to the grain boundaries and these are weaker than the  $\delta$  \* strengthened matrix.

### Conclusions

- (1) The primary strengthening phase in alloy 718 is body centred tetragonal, designated  $\delta$  \* Ni<sub>3</sub>Nb.
- (2) Creep ductility in alloy 718 is directly related to the amount of intergranular delta precipitation since this gives rise to niobium depletion and hence grain boundary softening.
- (3) No loss of ductility occurs on thermal exposure at temperatures up to 650°C for times up to 10,000 hours.

### References

- (1) Eiselstein, H.L., 1965, ASTM STP 369, p62
- (2) Boesch, W.J. and Canada, H.B., 1969, J. of Metals, 21, (10), p34
- (3) Ya-Fang Han, Deb, P. and Chaturvedi, M.C., 1982, Met.Sci., 16, (12), p555.
- (4) Paulonis, D.F., Oblak, J.M. and Duvall, D.S., 1969, Trans. ASM, 62, (3), p611.
- (5) Chaturvedi, M.C. and Ya-fang Han, 1983, Met.Sci., 17, (3), p145.
- (6) Cozar, R. and Pineau, A., 1973, Met. Trans., 4, (1), p47.
- (7) Oblak, J.M., Paulonis, D.F. and Duvall, D.S., 1974, Met.Trans., 5, (1), p143

\* INCONEL AND NIMONIC are Trademarks of the Inco Group of Companies